

Coronal Temperature Profiles from the August 11, 1999 Solar Eclipse

¹ James M. Weygand, and ¹ Peter Wurz,

Short title: CORONAL TEMPERATURE PROFILES

Abstract.

From a measurement campaign in Szombathely, Hungary during the solar eclipse of August 11, 1999 photographs were obtained with a 1000 mm Meade Telescope and Minolta camera of which 15 were useful for further data analysis. By digitizing these images, radial white light intensity profiles of the Sun's corona are plotted for a "shell" of the corona, where this shell's distance from the Sun is determined by the exposure time of the image. Fitting this intensity profile with the luminosity function of Badalyan and Livshits [1986], and assuming all the white light comes from the Sun's light scattered off the coronal electrons, the temperature can roughly be determined for this shell of the corona. With longer exposures of the Sun's corona, coronal layers for larger distances from the Sun can be examined. By plotting the temperature derived in a coronal layer for four different layers (i.e., four different eclipse exposures times) a temperature profile of the corona can be derived from about 0.25 to 2.50 solar radii.

Introduction

The total solar eclipse of August 11, 1999 was a normal eclipse, except that it was the first across Europe in about 9 years. The last one occurred over sparsely populated Northern Europe July 22, 1990, and the previous one over central Europe was February 15, 1961. It is estimated that millions to tens of millions of people saw the eclipse because of the path through central Europe, and a large fraction of these obtained one or more photographs of the eclipse. With increased availability and the relatively low cost of photographic and telescopic equipment, a significant fraction of these people used either a large photographic lens (greater than 200 mm) or a telescope to capture the eclipse on film (or on a CCD imager). The purpose of this article is to inform the public that they can use these photographs to get temperatures and electron densities for the inner coronal layer in the Sun's atmosphere.

For a brief period during totality, two of the three atmospheric layers of the Sun (i.e., the photosphere, the chromosphere, and the corona) are visible. The second largest and second farthest solar atmospheric layer from the Sun's surface is the red chromosphere (i.e., 1400 km thick), which can only be captured with a very short exposure. The next highest, the thickest layer, and by far the most visible atmospheric layer during totality is the corona, which extends over 30 solar radii from the Sun. Within the magnified photographs, one can easily see the high temperature, high density interstream coronal regions (i.e., the bright, nearly radial streaks) and low temperature, low density coronal hole regions (i.e., the dark lanes between the interstream coronal regions). Figure 1 indicates where some of these regions can be found during the August 11 solar eclipse. The high temperature, high density interstream coronal regions generally have a temperature of about 1.4 MK, where MK stands for a million degrees Kelvin, and a density around 2.0×10^{14} electrons m^{-3} . The low temperature, low density coronal hole regions typically have a temperature around 0.9 MK and a density around 0.9×10^{14} electrons m^{-3} .

There are approximately four different light sources which contribute to the

luminosity of the corona. These sources are:

- the K-(Kontinuierlich) corona,
the light reflected off the electrons.
- the F-(Fraunhofer) corona,
the light reflected off dust in the corona.
- the E-(Emission) corona,
the light emitted by the excited plasma.
- and the T-(Thermal) corona,
the infrared light emitted by dust.

By far the largest contributor within 1.3 solar radii of the surface comes from the Kontinuierlich corona. For this study we will assume that all the light photographed comes from the Kontinuierlich corona. Then next largest contributor to the coronal light is from the Fraunhofer corona and this light is not a large contribution until about 1.3 solar radii. Since the Emission and Thermal corona are such small sources of coronal light they will not be consider any further.

Instrumentation

The photographs for this study were obtained with a 1000 mm Meade Schmidt Cassegrain telescope, which has an opening of about 100 mm and a F-stop of about 10. The camera used was a Minolta X-370 manual camera. A cable release was attached to the camera to limit the amount of instrument vibration. The film used to record the images was AGFA professional ISO 50 color film. From first contact to last contact, 15 photographs were obtained and the exposure time varied from 1/500 second to 1 second.

Theory

For this study an adapted version of the theory from Badalyan and Livshits [1986] for the polarized luminosity of the corona has been used. This theory approximates

the corona with a hydrostatic electron density distribution at a constant electron temperature, T . Essentially, this means the entire corona, consisting mainly of free electrons, is assumed to be at one constant temperature, and the atmosphere's density decreases exponentially as the altitude from the surface of the Sun increases. For a recent review of the measured density profiles see Wurz and Gariel, 1999. With this assumption, the electron density can be approximated with the expression:

$$n(r) = n(R_{\odot}) \exp \left[-\frac{\mu m_H g_{\odot} R_{\odot}^2}{k_B T} \left(\frac{1}{R_{\odot}} - \frac{1}{r} \right) \right] \quad (1)$$

where $n(R_{\odot})$ is the electron density at the surface of the Sun, R_{\odot} is the radius of the Sun, μ is the mean molecular weight, m_H is the mass of hydrogen, g_{\odot} is the gravitational acceleration of the Sun at the surface, and k_B is Boltzmann's constant.

A full derivation of the Badalyan and Livshits equation for the polarized luminosity of the corona is beyond the scope of this study and we refer you to the following studies (Badalyan and Livshits, 1986; and Badalyan, 1986) for a more detailed derivation. The equation obtained in those two studies for the polarized luminosity is:

$$B(\rho) = \left(\frac{\pi \sigma B_{\odot} R_{\odot}^2}{2 \rho} \right) \left[n(R_{\odot}) \exp \left(\frac{\mu m_H g_{\odot} R_{\odot}}{k_B T} \right) \right] \left(1 + \frac{\beta^2}{2^2} + \frac{\beta^4}{2^2 4^2} + \frac{\beta^6}{2^2 4^2 6^2} + \dots \right) \quad (2)$$

where B is the luminosity, β is $\left(\frac{\mu m_H g_{\odot} R_{\odot}^2}{\kappa T} \right) / \rho$, σ is the Thompson scattering coefficient calculated per single free electron, and B_{\odot} is the mean luminosity of the solar disc. The independent variables (the values the astronomer knows) in equation (2) are r and B and the dependent variables (those values the astronomer is trying to find) in the equation are $n(R_{\odot})$ and T .

In summary, the equation (2) requires a number of values, which are mostly known constants that can be obtained from any first year astronomy book. A more difficult value to obtain is the mean luminosity of the solar disc for the day of the solar eclipse. Fortunately, the mean luminosity of the Sun can be found on the Internet at: <http://www.ngdc.noaa.gov/stp/SOLAR/IRRADIANCE/erbs.html>. The goal for this

study is to fit the Badalyan and Livshits theory (equation (2)) to the luminosity derived from the photograph in order to determine the electron density at the solar surface, as well as the temperature of the corona at a specific distance. The specific distance depends on the portion of the corona captured in the photograph. Short exposures of the corona during the eclipse capture details of the corona close to the solar surface, leaving the outer corona region black or dark due to the decreased luminosity there. Longer exposures capture details in the corona far from the solar surface, while leaving the inner portion of the corona over-exposed.

Two additional assumptions have been made for the interpretation of the measurements. Firstly, we assumed for this study that all the light recorded in the photograph originates from the K corona as noted in the introduction section. While this may seem like a large assumption it is a reasonable assumption within 1.3 Solar radii of the Sun's surface, and the difference is as small as 3% close to the solar surface (Ichimaoto et al., 1996). Secondly, it is assumed that all the light captured in the photograph is polarized, since we apply equation (2) which has been derived for polarized light. A more detailed description of a method to measure only the polarized light from the K corona can be found in **The Solar Corona** by Golub and Pasachoff. The second assumption is essentially the result of a balance between the total eclipse time and the number of different exposure times. Several photographs of the polarized and unpolarized corona are required for each exposure time in order to remove the unpolarized light correctly. However, the total eclipse only lasts for a few minutes and several photographs at different exposure times are required to obtain the temperature profile. Since this large number of photographs (i.e., the polarized and different exposures together) is difficult to take without an automated system, the polarized photographs were not taken and a variety of different exposures were obtained instead.

Procedure

Once photographs of totality have been obtained these need to be converted into an electronic format, which can be done either at a local developer or with a negative scanner. It is important, however, to have the images scanned at the maximum resolution with an absolute color scale and converted into some high resolution file like a Tag Image File Format (TIFF) file. The absolute color scale is important to prevent excess subtraction of background and the “whiting-out” of the brightest portions of the image. These are factors which the astronomer himself should be able to control. The high resolution scan and high resolution file are necessary to limit the loss of data. Furthermore, in this study the images were converted to black and white (grey scale) TIFF files. While information is lost in this conversion, it simplifies the amount of work, and the color information is not necessary for this study. The resulting image will be in terms of Digitization Numbers (DN) per pixel assuming a TIFF file is used. For a normal TIFF file the DN varies between 0 and 255, where zero is a black pixel in the image and 255 is a white pixel.

The TIFF images will need to be converted into units of luminosity ($\mathbf{J/s}$). This is explained in two parts here. Most major film companies have technical data sheets readily available to the public. The AGFA film company kindly supplied us with the information needed for the professional ISO 50 film used in this study. Unfortunately, these are useful for converting the **Density** of the photographic negative to the **Lux-seconds**, which need only be multiplied by a constant conversion factor to get the luminosity. A conversion of DN to Density is also necessary, but this conversion is not readily available. A number of complex methods could be used to do this, but for this study a simple method was used. It is assumed in the Lux-second versus Density curve of the film company that the lowest Density plateau (i.e., lowest Lux second values) is equivalent to a DN of zero and that the highest Density plateau is equivalent to the Density of 255. Furthermore, to further calibrate the curve an addition point can be used if the mean DN number of the solar disc is known, as well as the mean luminosity

of the Sun on the day of the solar eclipse. The mean DN number of the solar disc can be obtained by taking a photograph of the Sun just before first contact (or just after last contact), converting that photograph into a TIFF file, and finding the average DN over the solar disc. The mean luminosity of the Sun can be found on the Internet at the URL address given in the theory section. With these three calibration points, as well as with the Density to Lux-second plot, a conversion from DN to luminosity can be established.

A much more reliable method would be to photograph a series of known luminosities on the same roll of film as the solar eclipse photographs at the exposure times used for the solar eclipse. This should produce a more reliable DN to luminosity conversion.

Once the images have been converted to luminosity, a radial slice of the luminosity can be extracted from the image and fit with the Badalyan and Livshits [1986] luminosity equation. A fit of equation (2) to the data should give a reasonable coronal temperature for the luminosity from the “shell” of the corona fit, as well as the electron densities at the Sun’s surface. At a specific angle to the western limb of the Sun, the fit to the data can be done for as many different exposure times as available to get temperatures at different distances from the Sun. In this study, four photographs are used, hence, there will only be four different temperatures at four different radial distances for each angle from the Sun’s western limb. The result should be a smooth radial temperature profile, where the derived temperatures should be on the order of 1.5 million degrees Kelvin. In addition to verifying the approximate temperatures with one another, another check of the results can be done by comparing the electron densities derived from all the fits. Each fit should approximately obtain the same electron density at the surface of the Sun no matter what the exposure time and this value should be on the order of 2.0×10^{14} electrons m^{-3} . Within this study, the electron density varied by a factor of four. More will be discussed on this topic in the results and discussion section. Once the temperatures and density have been found at one angle, this procedure can be repeated at all angles around the Sun to derive temperature profiles at any angle. Examples of the results for this study can be found in Figure 2.

Results and Discussion

Figure 2 gives the resulting electron temperatures and densities for four different exposure times of the August 11, 1999 solar eclipse. Along the base of each plot is the angle with respect to the Sun's western limb in the photographs. Along the vertical axis of the top plot is the electron density at the surface of the Sun for the 1/60 second exposure of the eclipse. In the remaining four plots, all for increasingly longer exposure times, the vertical axis is the temperature in millions of degrees Kelvin. The exposure times are 1/250 sec, 1/60 sec, 1/8 sec, and 1 second and these exposure times correspond to shells of the corona center at $1.46 R_{\odot}$, $1.56 R_{\odot}$, $2.1 R_{\odot}$, and $2.69 R_{\odot}$. Recall that different shells of the corona are captured in the different photographic exposure times. The first item to notice is the repetition of some patterns in almost all of the temperature plots, for example, the coronal hole structure at about 240° . Furthermore, the electron density decreases (increases) at many of the same places as the decreases (increases) in the electron temperature, as one would expect for coronal holes (interstream regions). Finally, while many of the same structures are reproduced in the upper plots, these structures are not as evident in the bottom plot. This is most likely due to the smearing out and mixing of the corona by $2.69 R_{\odot}$. This can be more clearly observed in Figure 1, where the structures in the corona are not as sharp by $2.69 R_{\odot}$ from the center of the solar disc.

The second item to notice is the magnitude of the electron density. The mean density for this plot is 2.9×10^{14} electrons m^{-3} , which is well within the expected range of published values. See the study of Wurz and Gabriel [1999] for several examples. Previous values reported are as low as 1.5×10^{14} electrons m^{-3} , reported in the study of Guhathakurta et al. [1992], for the interstream region of the coronal atmosphere during solar minimum of the solar cycle, to as high as 5.0×10^{14} electrons m^{-3} , found in the study of Fludra et al., [1999] for the interstream region of the coronal atmosphere also during the solar minimum phase of the solar cycle. Coronal hole electron densities, which are expected to be smaller, are reported as low as 1.2×10^{13} electrons m^{-3} in the

study of Lantos and Avignon [1975] and as high as 3.0×10^{14} electrons m^{-3} within the study of Munro and Withbroe [1972]. Unfortunately, the electron density values found in this study significantly vary from photograph to photograph, which means there is a large uncertainty associated with the electron density of this study. For all four images examined in this study, the electron density varied by a factor of four, where as the values of previous studies vary by a factor of 2. Values as low as 0.7×10^{14} electrons m^{-3} to as high as 13.0×10^{14} electrons m^{-3} are found in this study. This large variation is not surprising, since the hydrostatic electron density distribution model is not perfect. It is well known in the solar physics community that the Sun is very dynamic and does not have a static atmosphere of a single temperature. While many careful scientific studies report a relative uncertainty on the order of 5% to 30%, the results from different authors vary by a factor of 2 or more. It is important to stress at this point that this study is by no means advanced in nature and that most of the electron densities found in this study are well within the range of previously report values.

The third item to notice in Figure 2 is the magnitude of the temperatures. The mean temperature in the first plot for the shortest exposure image of the solar eclipse is 1.7 MK at $1.46 R_{\odot}$ for the 1/250 second exposure, 2.4 MK at $1.56 R_{\odot}$ for the 1/60 second exposure, 2.2 MK at $2.10 R_{\odot}$ for the 1/8 second exposure, and 1.8 MK at $2.69 R_{\odot}$ for the last exposure. Typical temperatures for coronal interstream regions previously reported range from 1.0 MK to 2.1 MK at $1.46 R_{\odot}$ within the studies of Guhathakurta et al. [1999] and Bochsler [2000], 1.1 MK to 2.1 MK at $1.56 R_{\odot}$ within the studies of Guhathakurta et al. [1999] and Bochsler [2000], 1.0 MK to 1.65 MK at $2.1 R_{\odot}$ within the studies of Gibson et al. [1999] and Guhathakurta et al. [1999], and 0.8 MK to 1.5 MK at $2.7 R_{\odot}$ within the studies of Gibson et al. [1999] and Guhathakurta et al. [1999]. The study of Gibson et al. [1999] used polarized Kontinuerlich corona data taken at the High Altitude Observatory during solar minimum with the Mauna Loa coronagraph. A coronagraph is an instrument that creates an artificial solar eclipse inside the instrument. The data within the study of Bochsler [2000] is a model based on a fit to charge state equilibrium points within the corona for various elements

and an indirect measurement of the electron temperature. Finally, the data for the Guhathakurta et al. [1999] study was obtained from the spectral line intensities using the UVCS instrument on the SOHO spacecraft as well as the coronagraph instrument on the Spartan 201 spacecraft launched during shuttle missions. Both instruments obtained data during solar minimum. These previous values suggest that the ones in this study are higher than average, but still close to the expected magnitude. These results may be higher than average for several reasons:

- No polarization subtraction.
- No Fraunhofer corona subtraction.
- The solar cycle.

Recall from the procedure section that the Badalyan and Livshits equation is meant to apply to polarized light. This study did not use a polarizer, thus, there is an excess of luminosity found in the photographs. Within the studies of Badalyan [1986] and Koutchmy [1977] are published polarization values, which represent the fraction of the total light which is polarized in the corona at a specific distance from the Sun. These polarization values increase from 0.1 to 0.5 from the surface of the Sun to about 2 solar radii, which means the fraction of polarized light in the corona increases at larger distance from the solar surface to just after 2 solar radii. If this study were to take into account these polarization factors, then the amount of coronal luminosity would decrease at larger solar radii slower than observed in a radial plot of the intensity, which in turn would result in high temperatures for the longer exposures (i.e., coronal shells of larger radii). How much the temperature would increase is not clear at this time.

For point two above, one of the assumptions made for this study is that the majority of the coronal light comes from the Kontinuerlich corona. While this is generally true close to the solar surface, it is less correct farther from the solar surface. At approximately $2.3 R_{\odot}$, only 50% of the the total coronal luminosity comes from the Kontinuerlich corona (Koutchmy et al., 1978). Taking this fact into account would

reduce the amount of luminosity at larger distances from the solar surface and help to reduce the overall coronal temperature. How much the temperature would be reduced is, again, unclear. Nevertheless, the discussion on the temperature increase, due to the polarized light, combined with this discussion on the temperature decrease, due to the Fraunhofer coronal contribution, nearly results in a cancellation of the two effects. Quantitatively, there would be some increase in the temperature overall, but not a dramatic one.

The last reason the coronal temperatures in this study appear to be above average may be related to the solar cycle. The August 11, 1999 solar eclipse occurred during the increase of the solar cycle activity and the peak is expected to occur in late 2000 or early 2001. As the Sun becomes more active, it is also expected that the average temperature of the corona increases. This can be understood better by examining the number and scatter of coronal interstream regions, which are the hotter (1.5 MK) and more dense regions in the corona, as opposed to the coronal hole regions, which are less dense and cooler regions (0.9 MK). During solar minimum (i.e., a quiet sun) in images of the solar eclipse, there is generally two interstream regions observed, both at the Sun's equator, and two large coronal holes at the Sun's poles. As the solar activity increases (i.e., an active Sun) so does the number and scatter of the interstream regions. See Figure 3 for a cartoon representation of the active and quiet Sun. If there are more interstream regions and less coronal hole regions, then the average temperature of the corona would be expected to increase. This concept has already been shown in a study by Leblanc and LeSqueren [1969], where it was shown the corona's temperature was about 1.1 MK at solar minimum and 1.8 MK at solar maximum.

Another item to notice from Figure 2 is the initial increase in the coronal temperature for the first few plots, then the decrease in coronal temperature. To better illustrate this observation see Figure 4. Within Figure 4 there are two different temperature profiles from this study plotted: the solid line represents the average of all the temperatures for each shell of the corona, and the dotted line is the temperature profile for a coronal hole. Also plotted in Figure 4 are the temperature profiles

reported in several other studies. These previous studies indicate the variability of the temperature as well as the variability of the temperature profile's shape. Furthermore, displaying the profiles of other studies indicates that the temperature maximum within the figure for this study is not unexpected. However, why the temperature begins to sharply rise above the photosphere to maximum within the corona is still not known to solar physicists. Previous studies have found the peak temperature located as close as $1.26 R_{\odot}$ with a maximum of 2.2 MK within the study of Bochsler [2000] and as far as $2.1 R_{\odot}$ with a maximum of 1.67 MK (at solar minimum) within the study of Guhathakurta et al. [1999]. Based on four different studies, the mean location of the maximum coronal temperature is $1.8 R_{\odot}$. The four temperature plots of this study together suggest that the maximum coronal temperature is located between $1.56 R_{\odot}$ and $2.1 R_{\odot}$ and exceeds values of about 2.4 MK. The location of the corona temperature maximum of this study appears to be close to previously published values, but the peak temperature appears to be higher than all the previous studies examined here. The reason for this larger corona temperature maximum may be related to the assumptions already discussed or may be due to the fact that this study was performed closer to solar maximum than previous studies, which were mainly done near solar minimum.

One last item to discuss is the temperature within the coronal holes observed in the August 11, 1999 solar eclipse photographs. As stated in the introduction, the coronal hole's temperature is generally around 0.9 MK, but Figure 2 does not have any temperatures that low. However, there are some significant drops in the temperature, which can be related to coronal holes. These drops occur at about 70° , 115° , and 240° with respect to the western limb in the photograph, but are only a few degrees wide. Typical coronal holes span much larger areas on the solar surface. The reason the temperature does not decrease to around 0.9 MK is most likely related to the solar maximum phase in the solar cycle. As discussed, there are many more active regions scattered all over the Sun's surface closer to solar maximum. These regions are constantly throwing hot gases away from the Sun. Many of these hot streams cross in front of the cooler coronal hole regions, from the point of view of an observer on

Earth. Which means, there are hot layers in front of cool coronal hole layers and more hot layers behind the coronal hole. When the picture is taken, those regions cannot be easily differentiated and the result is known as *a line of sight effect* which leads to the higher temperatures observed in the coronal holes. To remove the line of sight effects is complex and beyond the scope of this study.

Conclusion

The purpose of this study is to give amateur astronomers the opportunity to obtain data from their photographs and show that their results are similar to professional solar physicists conclusions. In general, it is clear from the discussion that reasonable temperature profiles can be derived from careful analysis of August 11, 1999, solar eclipse photographs. In this study, temperature profiles are derived using four photographs and are obtained at all angles around the Sun with an uncertainty of 30%. The large uncertainty is the result of a large background, various assumptions about the corona, and due to pixel smearing from telescope motion. While the temperatures found are higher on average than previous published studies, those studies were more detailed and primarily done during Solar minimum, when the corona is less active (i.e, less heated). In addition to temperatures, electron densities were derived for the solar surface. The mean electron density derived from all photographs at all angles is 4.0×10^{14} electrons m^{-3} and lies within the range of previously published electron densities for both solar maximum and solar minimum. Furthermore, previously accepted electron densities have been observed to vary by a factor of 2 from study to study. Unfortunately, the electron densities found here vary by a factor of 4 between all the photographs. This variation is not critical since this study is by no means advanced in nature and most of the electron densities and temperatures found in this study are within the range of previously report values and exhibit patterns similar to previous studies.

While it is not necessary, the results for future studies can be improved in several ways. The most significant improvement could be made by using a CCD imager instead

of a camera. This would make the conversion from DN to luminosity considerably easier. The second significant improvement would be to use polarizing filters during the eclipse, however, this option is more difficult due to time constraints during the eclipse. With the implementation of these two improvements the amateur astronomer can begin to compete with the professional solar physicist. We strongly encourage similar studies by amateur astronomers to help verify professional astronomers results, to promote a competitive atmosphere, and to help bridge a gap between the public and the professional solar physics community.

Acknowledgements

The Swiss National Science Foundation for partial financial support in this study. L. Duvet at Centre d'Etudes des Environnements Terrestres et Planetaires for the invitation to Szombathely, Hungary. Lastly, we would like to also thank R.B. Lee and R.S. Wilson with Earth Radiation Budget Satellite for providing the solar irradiance value for the day of the solar eclipse.

References

- Badalyan O.G., Polarization of white-light corona under hydrostatic density distribution, *Astron. Astrophys.*, **169**, 305–312, 1986.
- Badalyan, O.G., and M.A. Livshits, The K-corona under hydrostatic density distribution: relevance to solar wind, *Solar Physics*, **103**, 385–392, 1986.
- Bochsler, P., Abundances and charge state of particles in the solar wind, *Rev. Geophys.*, **38**, 247–266, 2000.
- Fludra, A., G. Del. Zanna, D. Alexander, and B.J.I. Bromage, Electron density and temperature of the lower solar corona, *J. Geophys. Res.*, **104**, 9709–9720, 1999.
- Gibson, S. E., A. Fludra, F. Bagenal, D. Biesecker, G. Del Zanna, and B. Bromage, Solar minimum streamer densities and temperatures using whole Sun month coordinated data-sets, *J. Geophys. Res.*, **104**, 9691–9699, 1999.
- Guhathakurta, M., G.J. Rottman, R.R. Fisher, F.Q. Orrall, and R.C. Altrock, Coronal density and temperature structure from coordinated observations associated with the total solar eclipse of 1988 March 18, *Astrophys. J.*, **388**, 633–643, 1992.
- Guhathakurta, M., A. Fludra, S. E. Gibson, D. Biesecker, and R. Fisher, Physical properties of a coronal hole from a coronal diagnostic spectrometer, Mauna Loa Coronagraph, and LASCO observations during the whole Sun month, *J. Geophys. Res.*, **104**, 9801–9808, 1999.
- Leon Golub and Jay M. Pasachoff, *The Solar Corona*, Cambridge University Press, 1998.
- Ichimoto, K., H. Hara, A. Takedo, K. Kumagai, T. Sakurai, T. Shimizu, and H.S. Hudson, Measurement of the coronal electron temperature at the total solar eclipse on 1994 November 3, *Publ. Astron. Soc. Japan*, **48**, 545–554, 1996.
- Koutchmy, S., Study of the June 30, 1973 trans-polar coronal hole, *Solar Physics*, **51**, 399–407, 1977.
- Koutchmy, S., P. Lamy, G. Stellmacher, O. Koutchmy, N.I. Dzubenko, V.I. Ivanchuk, S.

Popov, G.A. Rubo, and S.K. Vsekhsvjatsky, Photometrical analysis of the June 30, 1973 solar corona, *Astron. Astrophys.*, **69**, 35–42, 1978.

Leblanc, Y., and A.M. Lequeren, Dimensions, temperature and electron density of the quiet corona, *Astron. Astrophys.*, **1**, 239–248, 1969.

Munro, R.H., and G.L. Withbroe, Properties of a coronal “hole” derived from extreme-ultra observations, *Astrophys. J.*, **176**, 511–520, 1972.

Wurz, P. and A.H. Gabriel, Wind acceleration processes, SOHO 8 Workshop Proceedings, Plasma Dynamics and Diagnostics in the Solar Transition Region and Corona, ESA SP-446, 87–95, 1999.

James Weygand, Physikalisches Institut, Universität Bern, Sidlerstrasse 5, CH-3007 Bern, Switzerland

Received March, 2000; revised 2000; accepted 2000.

¹Physikalisches Institut, Universitaet Bern

To appear in *Orion*, 2000.

Figure 1. This figure is a typical 1/4 second exposure photograph of the August 11, 1999 solar eclipse. Indicated in the image is a radial slice of the coronal intensity at the western limb of this photograph. The intensity within the “slice” would be fit with the equation from the theory of Badalyan and Livshits [1986]. After fitting this slice of the intensity, additional slices can be taken at all angles around the Sun. Also, indicated is a coronal hole region and coronal streamer within the solar atmosphere, as well as a good region to determine the background intensity.

Figure 2. This figure indicates the electron densities determined from one of the August 11, 1999 solar eclipse photographs, as well as the temperature determined from all of the photographs at all angles around the Sun. These angles are determined from the Sun’s western limb in the photographs. From top to bottom the exposure times for all of the temperature plots are 1/250 second, 1/60 second, 1/8 second, and 1 second. Given in the upper right hand corner of each plot is the mean value over all angles. Also, given in either the upper right corner or lower right corner of each plot is the mean distance of the coronal shell analyzed. Note that the large dip in the temperature at about 240° corresponds to the coronal hole indicated in Figure 1.

Figure 3. This figure is a cartoon schematic of the coronal structure during an active Sun and a quiet Sun. The top figure is a cartoon of the August 11, 1999 active solar corona. The red arrows indicate only a few of the interstream regions and the blue arrows point to two clear coronal holes. The bottom figure displays a simple coronal structure with two interstream regions at the Sun’s equator and two coronal hole regions at the Sun’s poles.

Figure 4. This figure gives the temperature profiles as determined in this paper and in other more sophisticated studies. The solid line is the temperature profile based on the mean temperature of each temperature versus angle plot at the mean distance of the fit from the Sun. The dotted line is the coronal hole temperature profile at an angle of 233° to the western limb of the Sun in the photograph. The coronal hole temperature profile has been shifted about $0.05 R_\odot$ to the right to better display the profile. The *B* stands for the results from the study of B for Badalyan, [1986], the *K* stands for the results from the study of Koutchmy et al. [1977], the + stands for the X-ray telescope results from the study of Fludra et al. [1999], and the * stands for the SOHO/CDS results from the study of Fludra et al. [1999]. The dash-dot line is a plot of the model from Bochsler [2000], the dash-dot-dot line is the measurements obtained from the study of Gibson et al., 1999, and the dashed line is a plot of the Guhathakurta et al. [1992, 1993] study's results.

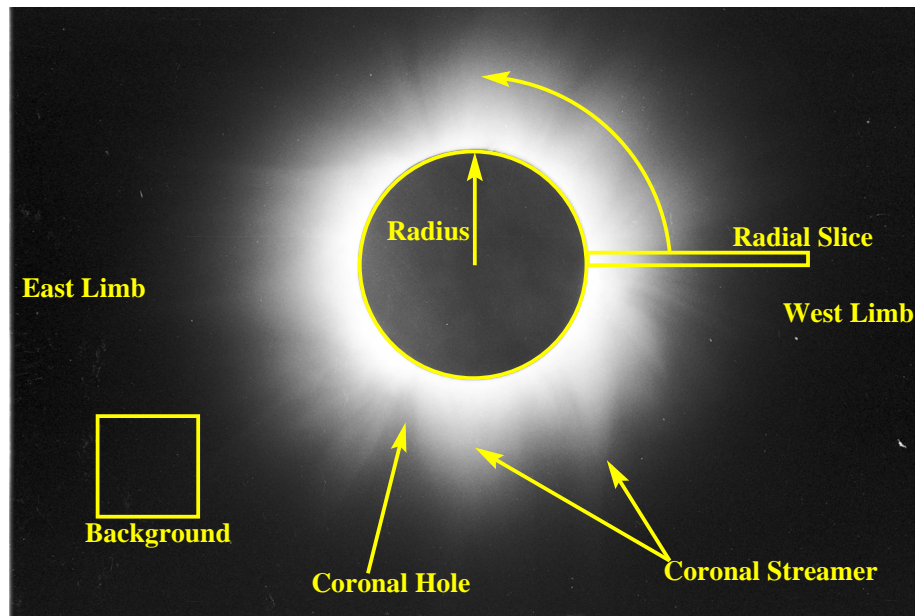


Figure 1.

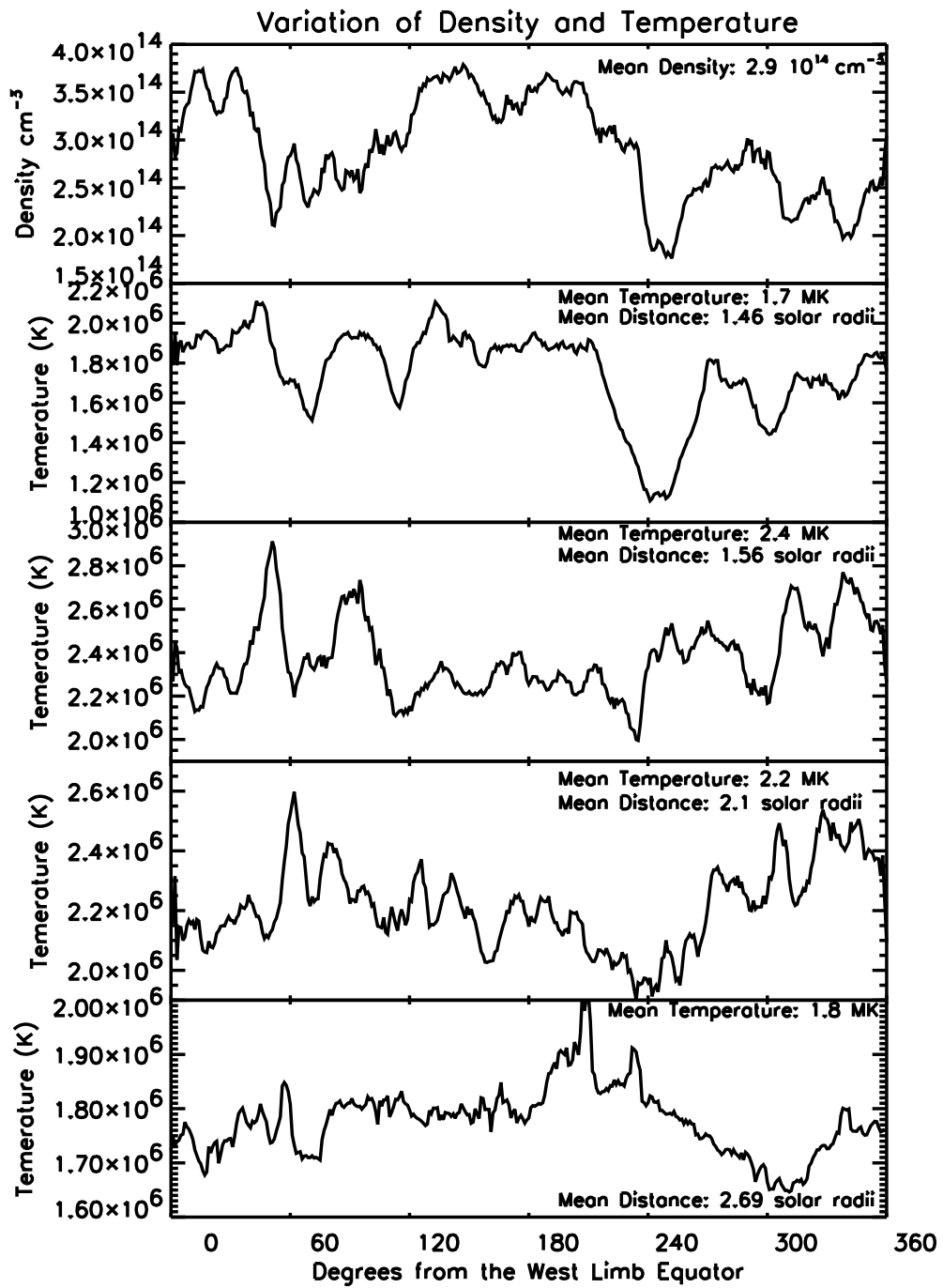


Figure 2.

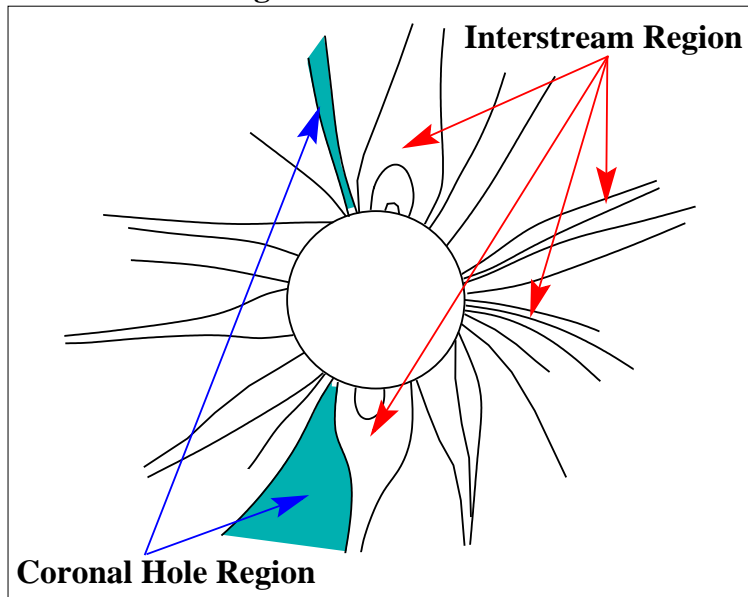
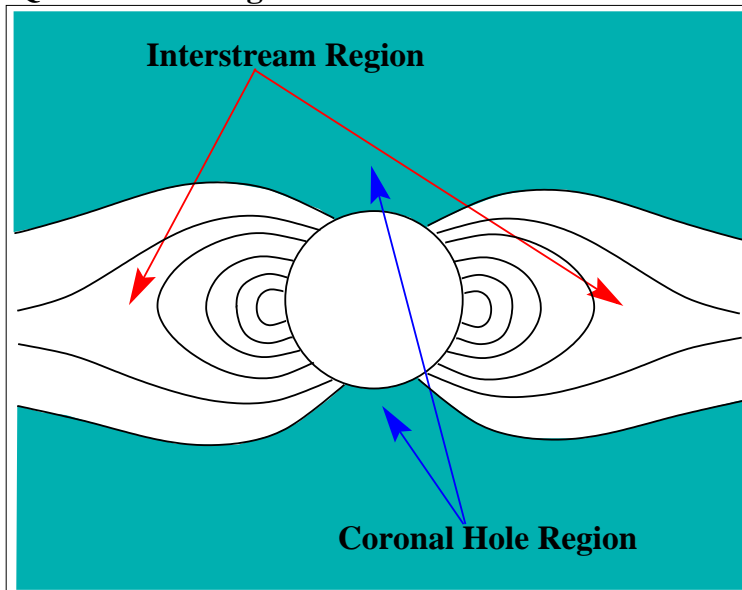
Active Sun during Solar Maximum**Quiet Sun during Solar Minimum**

Figure 3.

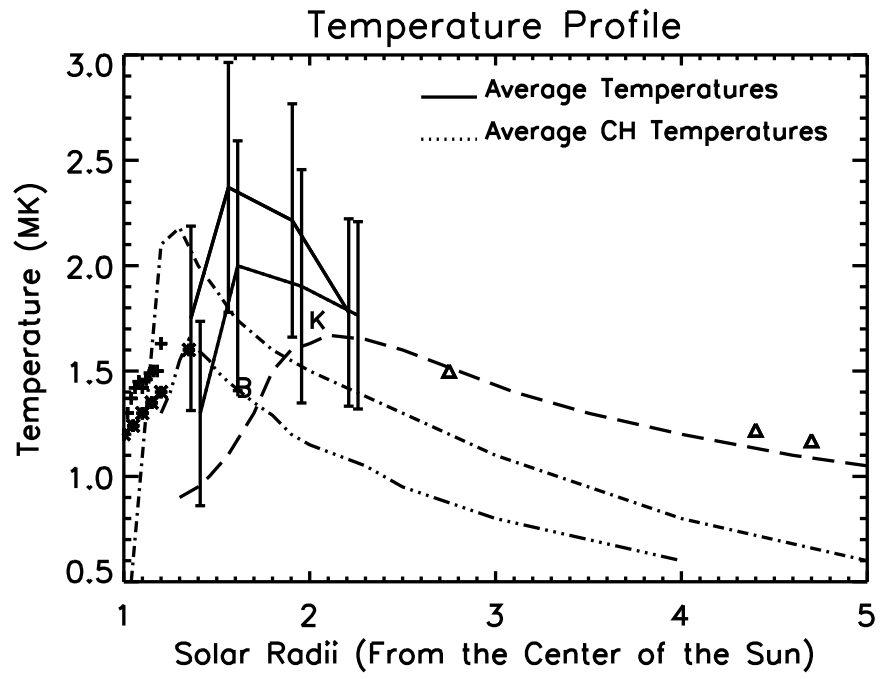


Figure 4.